

Ce³⁺ Centres in YAlO₃ (YAP) Single Crystals

Tetsuhiko TOMIKI, Hirokatsu ISHIKAWA, Tomoji TASHIRO,
Moritaka KATSUREN, Akira YONESU, Tatsuya Hotta,
Tsuyoshi YABIKU, Michihiro AKAMINE, Tomoyoshi FUTEMMA,
Tsuyoshi NAKAOKA and Isamu MIYAZATO

Department of Physics, Faculty of Science, University of the Ryukyus,
Nishihara, Okinawa 903-01

(Received March 30, 1995)

Spectra of optical absorption (3 eV ~ 6 eV) and emission (2.9 eV ~ 4.1 eV) have been investigated on Ce³⁺ centres in YAlO₃:Ce³⁺ single crystals at 297 K; excitation spectrum for 360 nm light in the Ce³⁺ emission band region has also been measured in the region of 3.5 eV ~ 6.2 eV. Measurement of excitation spectrum for Ce³⁺ centres in YAlO₃:Ce³⁺ powder phosphor has been made at room temperature in the region of 3 eV ~ 11 eV. The excitation spectra in the air UV region consist of five bands assignable to the five levels of the Ce³⁺ 5d; they are expressible by Gaussian functions, respectively, and therefrom the crystalline field splitting $10Dq = 1.12_8$ eV is derived. The excitation spectrum in the VUV region has a great peak at 8.05 eV which originates from the valence-band excitons. It is confirmed that the luminescence band expressed in terms of quanta per unit photon-energy interval can be fitted by two Gaussian components.

[optical absorption, emission and excitation spectra of Ce³⁺ of YAP:Ce³⁺, the air and vacuum UV regions]

§1. Introduction

Weber *et al.* found in 1969 that large high-quality single crystals of YAlO₃ suitable for laser rods can be grown easily using the Czochralski technique.¹⁾ YAlO₃ crystallizes in a slightly distorted perovskite structure with an orthorhombic unit cell and is called yttrium aluminate perovskite (YAP). Optically, it is a negative biaxial crystal. Trivalent rare-earth ions enter the YAlO₃ lattice substitutionally at Y³⁺ sites (C_{1h} symmetry) and trivalent transition-metal ions at Al³⁺ sites (C₁ symmetry). Optical spectra of these trivalent ions in YAlO₃ have been subjects of active investigations.

Spectroscopic studies on Ce³⁺ centres in YAlO₃ single crystals were carried out by Weber²⁾ and the results relevant to the present work are summarized as follows:

A Ce³⁺ ion with the electronic configuration 4f¹ has ²F_{7/2} and ²F_{5/2} manifolds as the ground states; the deeper manifold ²F_{5/2} is occupied with an electron and the manifold ²F_{7/2} is almost empty at room temperature. Optical

absorption bands due to the electronic transitions from ²F_{5/2} to ²F_{7/2} of Ce³⁺ in YAlO₃:Ce³⁺ were observed at 4.9 μm (0.25₈ eV), 4.0 μm (0.31₀ eV), 3.7 μm (0.33₅ eV) and 3.1 μm (0.40₀ eV). The 5d levels of Ce³⁺ at the lattice site of C_{1h} symmetry split into five levels. The optical absorption spectrum due to the electric dipole transitions from 4f to 5d levels shows four peaks at 303 nm (4.09 eV), 290 nm (4.27₅ eV), 275 nm (4.50₉ eV) and 238 nm (5.20₉ eV), respectively. Luminescence due to 5d → 4f transitions was observed as an emission band peaking at ~365 nm (3.40 eV) in the region of 330 nm ~ 400 nm. No structure was revealed in the emission spectrum, though the luminescence terminates on Stark levels of ²F_{5/2} and ²F_{7/2} manifolds. The Stokes shift of the f-d absorption and emission bands was estimated as ~4500 cm⁻¹ (0.558₀ eV). The decay of photo-excited Ce³⁺ luminescence was exponential with a life time of 1/e, $\tau_{1/e}$, of 16 nsec at 300 K. The excitation spectrum for the luminescence from Ce³⁺ confirmed the four features in the absorption spectrum and an additional peak at ~220 nm (5.63₆ eV) which

was not evident in the absorption spectrum. These five bands were assigned to the 5d levels of Ce³⁺.

Powder phosphor YAlO₃:Ce³⁺ excited by 20 nsec pulsed electron beam luminesces in the same spectral region as UV excited single crystals, and $\tau_{1/e} = 17 \sim 18$ nsec was measured for the fastest decay component.^{3,4)} Deterioration under an electron beam bombardment (c.w.) is not serious to the powder phosphor YAP:Ce³⁺ as compared to P47 phosphor (Y₂SiO₅:Ce³⁺). Hence the powder phosphor YAP:Ce³⁺ will be suitable for the application to flying-spot scanner tubes and beam-indexing tubes.

A sharply rising absorption below 200 nm (≈ 6.20 eV) had been regarded as the fundamental absorption edge of YAlO₃ characteristic of band-to-band transitions^{2,5)} until Abramov and Kuznetsov interpreted a steep rise of the absorption observed with natural light at $7.6 \sim 7.7$ eV as the onset of the fundamental absorption.⁶⁾ The spectra of absorption and reflectivity of YAP single crystals measured with linearly polarized lights confirmed that the sharply rising absorption near 6.2 eV is due to impurities and the steep rise at ~ 7.6 eV is the onset of the fundamental absorption of YAlO₃.⁷⁻⁹⁾

In this paper is shown first the excitation spectrum for light at 360 nm in the Ce³⁺ emission band region of powder phosphor YAP:Ce³⁺ in the region of 3.5 eV \sim 11.1 eV. The spectral behaviour is found to be consistent with the interpretation on the fundamental absorption onset described just above. Next, the spectra of absorption, luminescence and excitation for the Ce³⁺ centres of YAP:Ce³⁺ single crystals at room temperature are measured with natural light in the spectral region of 3.0 eV \sim 6.2 eV on the lower energy side of the fundamental absorption onset. The excitation spectrum is found to be expressible with five Gaussian bands, and their peak positions are in agreement with those given by Weber, respectively.²⁾ The absorption spectrum shows the features at the positions assignable to the four lower-energy Gaussian peaks of the excitation spectrum. The luminescence band is also expressible with two Gaussian bands, but no final determination of these two

components has been achieved because information on their intensity ratio is lacking.

Descriptions are given on experimental methods in §2, results in §3 and discussion in §4.

§2. Experimental Methods

Single crystals of YAlO₃:Ce³⁺ used were grown in the atmosphere of pure nitrogen by the Czochralski technique in the Nippon Electric Corporation, NEC, from the melt of mixture of the ingredient powders



here, $x \equiv [Ce^{3+}]_M = 0.03 \times 10^{-2}$. Ce³⁺ concentration incorporated into YAP lattice, $[Ce^{3+}]_L$, is unknown. All samples were mechanically cut and polished in the shape of plates of sizes of 14×7 mm² \times d , followed by chemical etching in hot H₃PO₄ to remove the surface layer of distorted lattice. Here, $1 \text{ mm} \geq d \geq 0.1 \text{ mm}$, d being the thickness.

Powder phosphor YAP:Ce³⁺ was prepared by heating the mixture (1) fluxed by powders of (BaF₂ + BaCO₃) at 1200°C for 4 hrs at the Matsushita Research Institute Tokyo, Inc.,^{3,4)} here, $[Ce^{3+}]_M = 0.5 \times 10^{-2}$. Single phase phosphor YAP:Ce³⁺ is obtainable by washing the product in HNO₃ solution to remove small amount of coexistent phase of BaAl₂O₄.

Measurements of absorption spectra in the visible and air UV regions were carried out by a Hitachi automatic recording double grating spectrophotometer 330 or by a Jobin-Yvon concave holographic grating (1200 lines/mm) monochromator H-20UV combined with a light chopper (Model 125A, EG & G Princeton Applied Res.), lock-in amplifier (Model 5101, EG & G Princeton Applied Res.), photomultiplier tube (Hamamatsu Photonics R955) and XY-recorder. In the latter, a Hanau HS-D200F D₂ lamp (100–200 W) was mainly used as a light source in the air UV region. Reflectivity and absorption spectra of single crystalline specimens in the VUV region were measured by Seya-Namioka type VUV grating monochromators (1200 lines/mm, spectral slit width $\Delta\lambda \approx 2.5$ Å); the light source was a conventional hydrogen discharge lamp or the plane polarized synchrotron radiation.

Spectra of luminescence from single crystal-

line samples of YAP:Ce³⁺ excited with the light at 290 nm from the Hanau HS-D200F D₂ lamp were measured by the system of a Jobin-Yvon monochromator (set to $\Delta\lambda \approx 2.5$ nm or 1.25 nm) described just above (the schematic block diagram of the apparatus for the measurement was given in Fig. 1¹⁰). Here, the Hanau D₂ lamp light was monochromatized by a Leiss double prism monochromator. Measurements of the excitation spectra for the Ce³⁺ luminescence were made by the R955 photomultiplier output for the light at 360 nm in the Ce³⁺ luminescence band region; in this case, the excitation light from the Hanau HS-D200F D₂ lamp was monochromatized by the Jobin-Yvon monochromator (set to $\Delta\lambda = 2.5$ nm or 1.25 nm) and the light of 360 nm by the Leiss double monochromator. In the above, a wavelength drive was achieved by the Jobin-Yvon monochromator. Measurements of the excitation spectra of the powder phosphor YAP:Ce³⁺ were made by use of light from the hydrogen discharge lamp monochromatized by the Seya-Namioka type monochromator.

Spectral energy distribution of the D₂- and H₂-lamps illuminating on sample surfaces were calibrated by use of the photoluminescence from sodium salicylate powder sprayed onto a glass slide for wavelengths $\lambda \lesssim 3000$ Å.

§3. Results

The excitation spectrum $Q(E)$ for the luminescence from Ce³⁺ centres in the powder phosphor YAP:Ce³⁺ is shown in arbitrary unit by data points, dots, and a broken curve in the region of 3 eV~11 eV in Fig. 1,¹¹ E being the photon energy. One notices a triplet (3.8 eV~4.8 eV) and two bands (at ~ 5.2 eV and ~ 5.6 eV) followed by $Q(E)$ of low magnitude tailing towards 7.3 eV. A part of $Q(E)$ consisting of the five bands in the region $E \lesssim 6$ eV arises from the 5d levels of Ce³⁺ ions.² A steep rise of $Q(E)$ occurs at ~ 7.5 eV and a peak at 8.05 eV, respectively. Beyond the peak, $Q(E)$ is nearly constant in magnitude in the region of 9 eV~11 eV. In order to understand the E -dependence of $Q(E)$ in the region of $E \gtrsim 7.5$ eV, the spectra of reflectivity $R(E)$ and the Kramers-Kronig analysed $\varepsilon_2(E)$, the imaginary part of the dielectric constant, are also displayed in Fig. 1 for $\langle a \rangle // E$, E being the

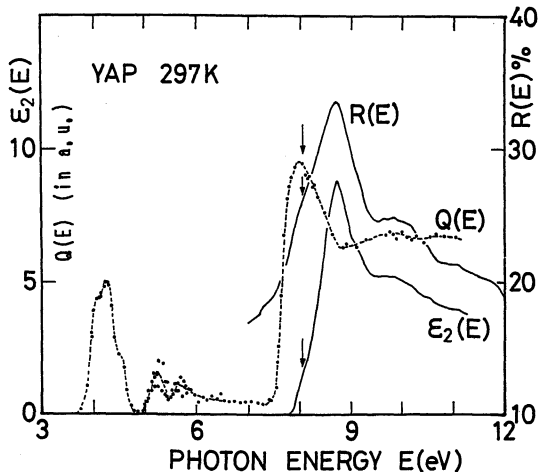


Fig. 1. The excitation spectrum $Q(E)$ for the Ce³⁺ luminescence ($\lambda \approx 360$ nm) in powder phosphor YAP:Ce³⁺ at 297 K, where dots stand for data points.¹¹ The spectra of $R(E)$ and $\varepsilon_2(E)$ of YAP single crystals at 297 K are shown for $\langle a \rangle // E$ in their intrinsic region for comparison.⁹ Arrows indicate locations of excitonic structures revealed on the spectra of $Q(E)$, $R(E)$ and $\varepsilon_2(E)$, respectively, see the text.

electric vector of light.⁹ Each of arrows indicates each of the spectral positions of the shoulders of $R(E)$ and $\varepsilon_2(E)$ and of the peak of $Q(E)$, respectively. The arrows are found to lie at almost the same photon energy. The onset of the steep rise of $Q(E)$ at ~ 7.5 eV coincides in position with that of the intrinsic absorption tail (cf. Fig. 2); the energy position of the arrows is nearly equal to that of the convergence point of the intrinsic absorption tails at various temperatures for each polarization of light.⁹ These observations indicate that the features marked with the arrows are related to the formation of excitons associated with electronic transitions from O²⁻ 2p⁶ valence to Y²⁺ 4p⁶(4d+5s) conduction bands.⁹ It is believed that the peak of $\varepsilon_2(E)$ at 8.65 eV and the subsequent features in the higher energy region arise mainly from the band-to-band transitions described just above. One sees that $Q(E)$ is greater in the intrinsic region than in the region related with the Ce³⁺ 5d levels.

The absorption spectra for single crystals at 297 K of YAP (a) and of YAP:Ce³⁺ (b) are shown by dots in Fig. 2 in terms of $\log_{10} A(E)$ [cm⁻¹] in the region of 3.0 eV~8.0 eV and 3.0 eV~6.2 eV, respectively, $A(E)$ being the

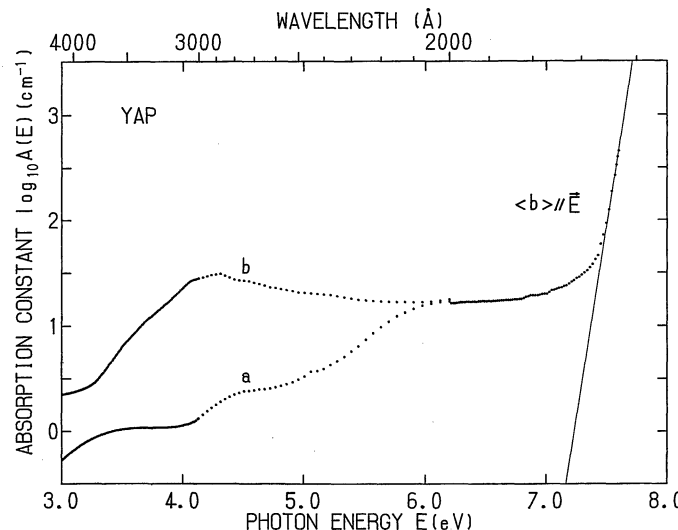


Fig. 2. The spectra of $\log_{10} A(E)$ of single crystals of YAP (curve a in the region of $3.0 \text{ eV} \sim 8.0 \text{ eV}$) and YAP:Ce³⁺ (curve b in $3.0 \text{ eV} \sim 6.2 \text{ eV}$) at 297 K. The data of $E \geq 6.2 \text{ eV}$ were measured with plane polarized light ($\langle b \rangle // E$) and a thinner line represents E -dependence of the intrinsic absorption tail of YAP.⁹ The data of $E \leq 6.2 \text{ eV}$ were taken with natural light.

absorption constant. The measurements of $A(E)$ for $E \leq 6.2 \text{ eV}$ were made with natural light and those for $E \geq 6.2 \text{ eV}$ with the plane polarized synchrotron radiation. $A(E)$ was derived from $T_r(E)$, the transmittance measured, by the equation

$$T_r(E) = [1 - R(E)]^2 \cdot \frac{\exp[-A(E)d]}{1 - R(E)^2 \cdot \exp[-2A(E)d]}; \quad (2)$$

here, $R(E)$ for $E \leq 6.2 \text{ eV}$ is calculated from the index of refraction¹²⁾ by use of the Fresnel's formula for reflectivity and $R(E)$ for $E \geq 6.2 \text{ eV}$ was given in ref. 9. A thinner line in Fig. 2 represents the photon-energy dependence of the intrinsic absorption tail of single crystals of YAlO₃ at 297 K for $\langle b \rangle // E$.⁹ Any absorption observed at 297 K on the lower energy side of this line is due to the presence of impurities (including imperfections) in the YAP lattice. The absorption spectra of $A(E)$ [cm^{-1}] for a and b are shown by dots in Fig. 3(A) and their difference $\Delta A(E)$ [cm^{-1}] in Fig. 3(B) both in the region of $3.0 \text{ eV} \sim 6.2 \text{ eV}$. Shoulders are seen on $\Delta A(E)$ at $\sim 4.1 \text{ eV}$, $\sim 4.5 \text{ eV}$ and $\sim 5.2 \text{ eV}$ and a peak at $\sim 4.3 \text{ eV}$. Figure 4 shows the excitation spectrum $Q(E)$

by dots for the light at $\lambda \approx 360 \text{ nm}$ in the Ce³⁺ luminescence band region of YAP:Ce single crystals ($d \approx 1 \text{ mm}$) at 297 K. The excitation spectrum carries the peak and shoulders at the same spectral positions as the absorption spectrum $\Delta A(E)$, respectively, and additionally a band at $\sim 5.6 \text{ eV}$ which is not evident in Fig. 3(B). These five structures are also nearly in agreement in their spectral positions with those found on the powder phosphor in Fig. 1.

The luminescence spectra from single crystalline specimens ($d \approx 1 \text{ mm}$) of YAP:Ce³⁺ at 297 K excited with the natural light at 290 nm are shown in Figs. 5(a) and 5(b). In Fig. 5(a), the apparent luminescence spectrum $B_{\text{em}}(\lambda)$, i.e., the spectrum recorded by the photomultiplier output is shown against wavelength λ . $B_{\text{em}}(\lambda)$ decreases rapidly in magnitude with the decrease in λ on the shorter wavelength side of the peak at $\lambda \approx 364 \text{ nm}$. This is caused by the self-absorption by the Ce³⁺ centres in the specimen, cf. Figs. 3 and 4. Correcting the self-absorption $\mathfrak{A}(\lambda)$, the luminescence spectrum $\Phi_{\text{em}}(E)$ expressed in quanta per unit photon-energy interval is converted from $B_{\text{em}}(\lambda)$ by the following equation:

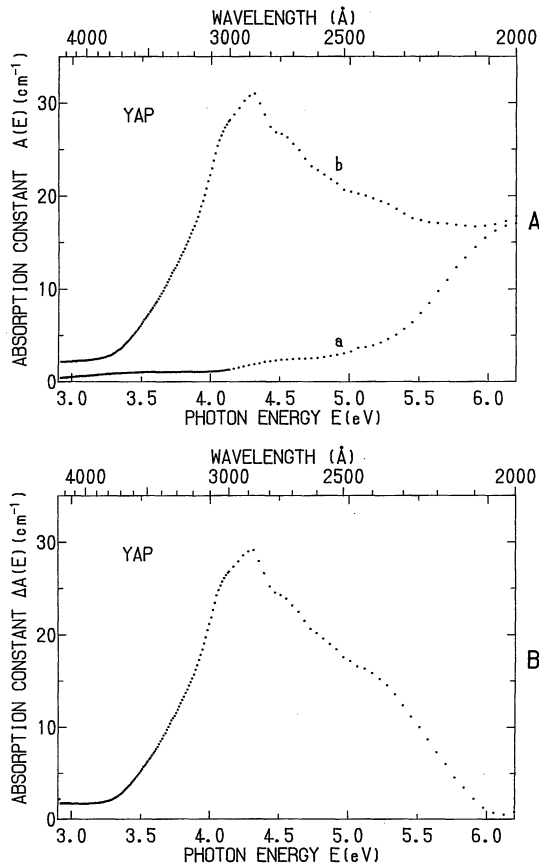


Fig. 3. (A) The absorption spectra, as represented by $A(E)$ vs. E , of single crystals of YAP (curve a) and YAP:Ce³⁺ (curve b). (B) The difference spectrum $\Delta A(E)$ as defined by $\Delta A(E) = A(E)$ for $b - A(E)$ for a .

$$\Phi_{\text{em}}(E) = C \frac{\lambda^3 B_{\text{em}}(\lambda)}{P(\lambda) M(\lambda) \mathfrak{A}(\lambda) [1 - R(\lambda)]}; \quad (3)$$

$$E = hc/\lambda.$$

Here, C is a proportionality constant, and $M(\lambda)$ the transmittance of the monochromator, Jobin-Yvon H-20UV, measured by a JAS-COSO-W030 W-incandescent lamp of a known colour temperature and a D₂ lamp (L544) of a known spectral energy distribution; $P(\lambda)$ is the photo-cathode emission sensitivity of the photomultiplier calibrated by the manufacturer. An explanation is given on the reflectivity $R(\lambda)$ of the specimen, cf. eq. (2). In our experimental arrangement of the apparatus (cf. Fig. 1¹⁰), $\mathfrak{A}(\lambda)$ is well described by the equation

$$\mathfrak{A}(\lambda) = \frac{A(\lambda)}{A(\lambda) + A(\lambda')} \times [1 - \exp \{-(A(\lambda) + A(\lambda'))d\}], \quad (4)$$

here, λ and λ' are wavelengths in the luminescence band region and at the excitation light, respectively. $\Phi_{\text{em}}(E)$ thus converted is plotted by dots against $E = hc/\lambda$ in Fig. 5(b). A fine feature of $\Phi_{\text{em}}(E)$ in the region of 376 nm (3.30 eV) ~ 364 nm (3.41 eV) originates from $M(\lambda)$. One notices that $\Phi_{\text{em}}(E)$ increases in magnitude with the decrease in E in the region of $3.6 \text{ eV} \geq E \geq 3.37 \text{ eV}$.

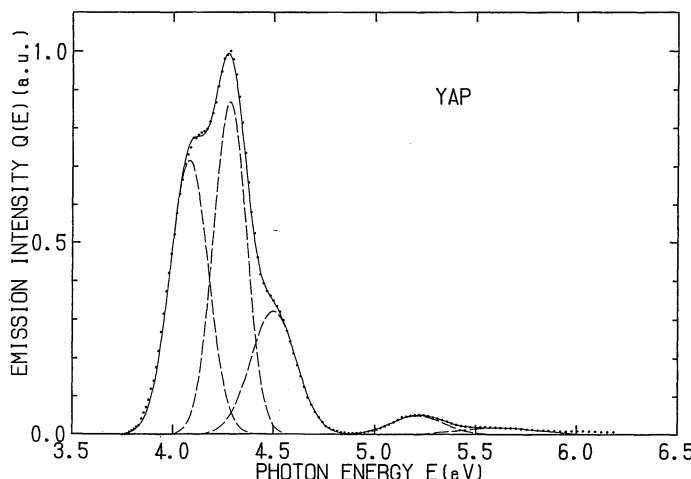


Fig. 4. The excitation spectrum $Q(E)$ for the Ce³⁺ luminescence (natural) light ($\lambda \approx 360 \text{ nm}$) of YAP:Ce³⁺ single crystals ($d \approx 1 \text{ mm}$) at 297 K. Dots stand for data points, broken curves for five Gaussian components for the best fit to the dots, respectively, and a full curve represents their sum.

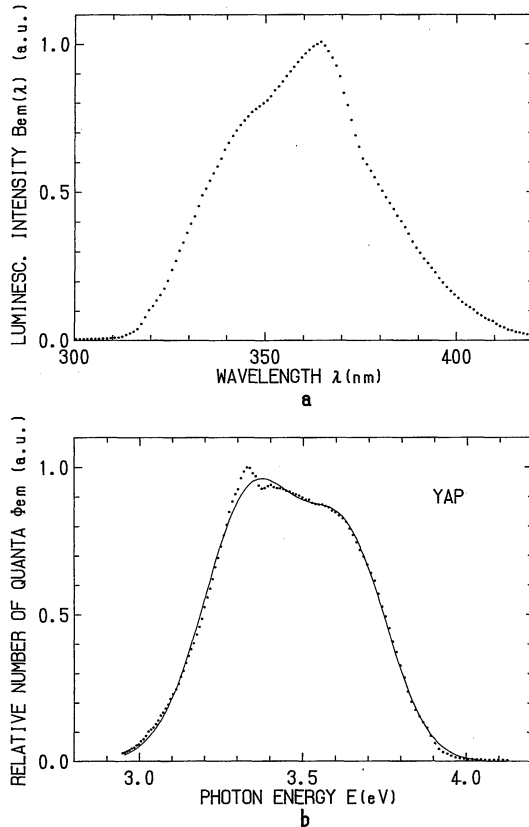


Fig. 5. (a) The apparent emission spectrum of Ce³⁺ centres of YAP:Ce³⁺ single crystals ($d \approx 1$ mm) at 297 K as represented by a photomultiplier output $B_{\text{em}}(\lambda)$ vs. wavelength λ . Dots stand for data points measured with a spectral slitwidth $\Delta\lambda = 1.25$ nm. (b) The emission spectrum $\Phi_{\text{em}}(E)$ converted from $B_{\text{em}}(\lambda)$ in Fig. 5(a) by eq. (3) and expressed in quanta per unit photon-energy interval. Dots stand for data points, and a thinner curve for the sum of two Gaussian components for the best fit to the dots, see §4.2. Fine structure seen in the region centred at ~ 3.35 eV arises from $M(\lambda)$ of the Jobin-Yvon H-20UV, cf. eq. (3).

§4. Discussion

4.1 Excitation spectrum $Q(E)$ related to the 5d levels of Ce³⁺

The triplet part of $Q(E)$ in Fig. 4 can be expressed by the Gaussian functions

$$G_j(E) = G_{0,j} \exp [-\beta_j(E - E_{\text{max},j})^2], \quad (5)$$

$$\beta_j = (2/B_j)^2 \ln 2,$$

here, $j=1, 2$ and 3 in the order of increasing $E_{\text{max},j}$; B_j stands for the full half value width of

Table I. The Gaussian parameters selected for the best fit to the excitation spectrum $Q(E)$ for the Ce³⁺ centres in YAP:Ce³⁺ single crystals. The Gauss function is defined by $G_j(E) = G_{0,j} \exp [-\beta_j(E - E_{\text{max},j})^2]$ with $\beta_j = (2/B_j)^2 \ln 2$, where $j=1, 2, \dots, 5$ in the order of increasing $E_{\text{max},j}$.

j	$E_{\text{max},j}$ [eV]	B_j [eV]	$G_{0,j}$ [a.u.]
1	4.080	0.2222	0.7198
2	4.282	0.1930	0.8734
3	4.500	0.2654	0.3241
4	5.210	0.3061	0.0499
5	5.620	0.4739	0.0182

$G_j(E)$. Three Gaussian bands (broken curves in Fig. 4) are calculated by eq. (5) with the use of the values of the parameters selected for the best fit to dots, the data points; the values are listed in Table I. The full curve in Fig. 4 represents the sum of these three bands and is found to be in excellent agreement with dots. The two bands, $j=4$ and 5 , lying in the higher energy region can also be expressed by the Gaussian functions by use of the values listed in Table I. To show this more clearly, the broken and full curves are plotted together with the experimental data on expanded scales in Fig. 6. The values of $E_{\text{max},j}$ are found to be in agreement with those given by Weber on his excitation spectrum, respectively (cf. §1).²⁾ Regarding the components of $j=1, 2$ and 3 as the d₆ and $j=4$ and 5 as d₅ of the 5d levels of Ce³⁺ in YAP, the crystalline field splitting 10Dq is calculated as 1.128 eV.

The difference spectrum $\Delta A(E)$ in Fig. 3(B) has the shoulders at $E_{\text{max},j}$ with $j=1, 3$ and 4 and the peak at $E_{\text{max},2}$ but has no suggestion for the peak at $E_{\text{max},5}$. In addition, $\Delta A(E)$ cannot be expressed only by those Gaussian functions which are specified with the values of $E_{\text{max},j}$ and B_j given in Table I and with appropriate values of $G_{0,j}$. Thus, the spectrum of $\Delta A(E)$ shown here represents photo-absorptions by Ce³⁺ as well as other unknown impurities.

4.2 Emission spectrum $\Phi_{\text{em}}(E)$

The emission spectrum $\Phi_{\text{em}}(E)'$ of powder phosphor YPO₄:Ce³⁺ consists of well separated two components peaking at 3.713 eV

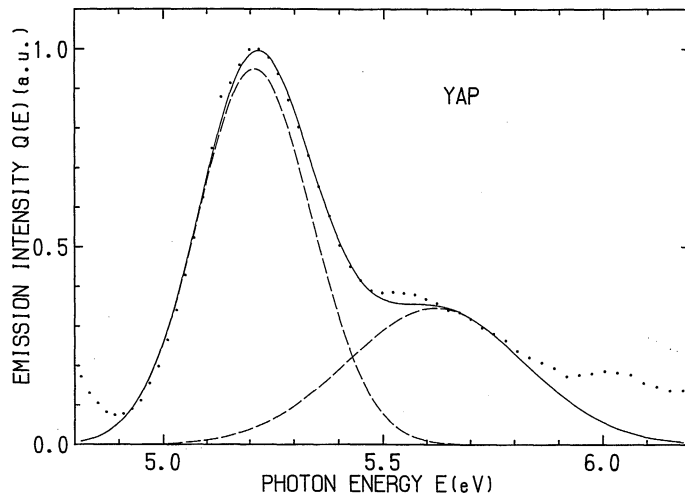


Fig. 6. The excitation spectrum $Q(E)$, a part of Fig. 4, plotted on expanded scales of coordinates in the $d\gamma$ region of the Ce^{3+} 5d of YAP:Ce³⁺ single crystals at 297 K. As regards dots, broken and thinner curves, see the caption of Fig. 4.

and 3.478 eV at room temperature; the photon-energy dependence of the lower energy component is found to be close to Gaussian shape.^{11,*} Here, $\Phi_{\text{em}}(E)'$ is the quantity derived from eq. (3) with putting $\mathfrak{U}(\lambda)=1$, because $\mathfrak{U}(\lambda)$ cannot easily be estimated for powder phosphors. We believe that in YPO₄:Ce³⁺ phosphor two Gaussian bands are formed respectively corresponding to photo-emitting transitions from the lowest d level to the two ground manifolds $^2F_{7/2}$ and $^2F_{5/2}$ of the Ce³⁺ centres. We imagine that similar phenomena occur in YAP:Ce³⁺ single crystals and these resulted in the emission band $\Phi_{\text{em}}(E)$ observed in Fig. 5(b). In fact, $\Phi_{\text{em}}(E)$ in Fig. 5(b) is expressible by two Gaussian components as shown by a full curve, a sum of the two components, which is in good agreement with experimental values, dots. An excellent fit by Gaussian components to each of $Q(E)$ and $\Phi_{\text{em}}(E)$ indicates that the configurational coordinate model is applicable to the Ce³⁺ centres in YAP.

The spectrum $\Phi_{\text{em}}(E)$ having no distinct indication for the two components such as

shown in Fig. 5(b) may be expressible with a number of Gaussian pairs. However, information on a ratio of the intensity (area) of the component of a Gaussian pair will help us to more easily discriminate the most probable Gaussian pair among the pairs which can reproduce $\Phi_{\text{em}}(E)$. For example, the full curve in Fig. 5(b) represents one of the possibilities which are obtainable under the condition that the intensity ratio of the two components should be close to the ratio of the multiplicity $2J+1$ of the final manifolds $^2F_{7/2}$ and $^2F_{5/2}$ for the photoemitting transitions, i.e., 4 : 3. In the above, $(E_{\text{max}}, B, G_0) = (3.342 \text{ eV}, 0.3372 \text{ eV}, 0.9312)$ and $(3.635 \text{ eV}, 0.3016 \text{ eV}, 0.7287)$ were selected as the Gaussian parameters. The peak separation 0.293 eV of the Gaussian pair selected in the above is found to be nearly equal to the mean value 0.32 eV for the separations between the crystalline Stark levels of $^2F_{7/2}$ and the lowest crystalline Stark level of $^2F_{5/2}$.²⁾ It is not certain, however, that such an intensity ratio has ever been theoretically justified for Ce³⁺ centres of YAP to our knowledge.

A spectral behaviour of the full curve indicates that $\Phi_{\text{em}}(E)$ increases in magnitude with the decrease of E towards $E \sim 3.38$ eV. This does not always experimentally guarantee that the lower-energy Gaussian component is

* The higher energy component is located closely to the excitation band peaking at 3.85 eV so that the band shape is distorted by self-absorption and depends on the Ce³⁺ concentration of the phosphor.

greater in intensity than the higher-energy one. The reason for this is as follows: $\Phi_{\text{em}}(E)$ for a Ce³⁺ luminescence band in YAG single crystals increases in magnitude with the increase in E towards $E \sim 2.23$ eV near the peak of the higher-energy Gaussian component.¹⁰ In this case, the spectrum $\Phi_{\text{em}}(E)$ is expressible with those Gaussian pair in which the lower-energy Gaussian component is greater in intensity than the higher-energy one, too.

It has been confirmed in this work that $\Phi_{\text{em}}(E)$ is expressible with two appropriate Gaussian components; at present, however, a final determination of the Gaussian pair is difficult to be made for $\Phi_{\text{em}}(E)$.

One of the authors, T. Tomiki, wishes to thank Dr. T. Miyata for his giving him access to experimental facilities, including the Hitachi automatic recording spectrophotometer 330, in the Matsushita Research Institute Tokyo, Inc. He is grateful to Dr. Y. Kuwano, Fundamental Research Laboratories, NEC Corporation, for his information on crystal growth of YAP single crystals. We are grateful to Mr. Junkoh Tamashiro for his plotting the figures in this paper.

References

- 1) M. J. Weber, M. Bass, K. Andringa, R. R. Monchamp and E. Comperchio: *Appl. Phys. Lett.* **15** (1969) 342. This reference also quotes *JETP Lett.* **9** (1969) 303 by Kh. S. Bagdasarov and A. A. Kaminskii reporting their stimulated emission at room temperature from a 3.5×30 mm rod of YAlO₃ containing 3 wt% Nd.
- 2) M. J. Weber: *J. Appl. Phys.* **44** (1973) 3205.
- 3) T. Timiki, T. Takeda, T. Miyata and F. Muramatsu: *Tech. Digest, Phosphor Res. Soc. 167th Meeting, 1977*, p. 10 [in Japanese].
- 4) T. Takeda, T. Miyata, F. Muramatsu and T. Tomiki: *J. Electrochem. Soc.* **127** (1980) 438.
- 5) M. J. Weber and T. E. Varitimos: *J. Appl. Phys.* **42** (1971) 4996.
- 6) V. N. Abramov and A. I. Kuznetsov: *Sov. Phys. -Solid State* **20** (1978) 399.
- 7) T. Tomiki, F. Fukudome, M. Kaminao, M. Fujisawa and Y. Tanahara: *J. Phys. Soc. Jpn.* **55** (1986) 2090.
- 8) T. Tomiki, F. Fukudome, M. Kaminao, M. Fujisawa, Y. Tanahara and T. Futemma: *J. Lumin.* **40 & 41** (1988) 379.
- 9) T. Tomiki, M. Kaminao, Y. Tanahara, T. Futemma, M. Fujisawa and F. Fukudome: *J. Phys. Soc. Jpn.* **60** (1991) 1799.
- 10) T. Tomiki, H. Akamine, M. Gushiken, Y. Kinjoh, M. Miyazato, T. Miyazato, N. Toyokawa, M. Hiraoka, N. Hirata, Y. Ganaha and T. Futemma: *J. Phys. Soc. Jpn.* **60** (1991) 2437.
- 11) T. Tomiki, T. Miyata, T. Takeda and F. Muramatsu: unpublished work at the Matsushita Research Institute Tokyo, Inc. (1977).
- 12) K. W. Martin and L. G. DeShazer: *Appl. Optics* **12** (1973) 941.